



## Phase formation in a Ni–50Cr HVOF coating

J. Saaedi <sup>a,b,\*</sup>, T.W. Coyle <sup>a</sup>, S. Mirdamadi <sup>b</sup>, H. Arabi <sup>b</sup>, J. Mostaghimi <sup>a</sup>

<sup>a</sup> Centre for Advanced Coating Technologies, Department of Materials Science and Engineering, University of Toronto, Toronto, Canada

<sup>b</sup> Department of Materials and Metallurgical Engineering, Iran University of Science and Technology, Tehran, Iran

### ARTICLE INFO

#### Article history:

Received 24 December 2007

Accepted in revised form 27 May 2008

Available online 13 June 2008

#### Keywords:

HVOF

Thermal-spray coatings

Ni–50Cr

Non-equilibrium phases

Sigma phase

### ABSTRACT

A complex, fine scale microstructure of non-equilibrium phases is obtained by HVOF deposition of Ni–50Cr alloy due to the rapid cooling experienced by the splats which make up the as-deposited coatings. XRD analyses indicated that the as-deposited coatings consisted predominantly of a single fcc  $\gamma$ -Ni phase. Two small peaks suggested the presence of NiO and/or NiCr<sub>2</sub>O<sub>4</sub> at the limit of detection (~5%). Shoulders on the main  $\gamma$ -Ni peaks were interpreted as evidence of a second, lower Cr content  $\gamma$ -Ni phase. Characterization of the oxide content of the as-deposited coatings by X-ray diffraction, image analysis of backscattered electron images, and electron probe microanalysis yielded conflicting results due to the size of the microstructural features present relative to the spatial resolution of these techniques. Due to the nature and feature size of the non-equilibrium oxide phase(s), direct measurement of the oxygen content by EPMA was found to be the most accurate technique. Heat treatment of an as-deposited coating at 650 °C in vacuum resulted in coarsening of the microstructural features, and an approach towards a mixture of equilibrium phases consisting of  $\gamma$ -Ni,  $\alpha$ -Cr, and Cr<sub>2</sub>O<sub>3</sub>. Evidence was also seen in the XRD pattern of an intermetallic  $\sigma$  phase that has previously only been reported in thin films of Ni–Cr alloys.

© 2008 Elsevier B.V. All rights reserved.

### 1. Introduction

Nickel–chromium alloys attract the attention of metal scientists by their high temperature corrosion properties [1]. The presence of chromium in the alloys results in formation of an oxide layer which reduces further oxidation and hot corrosion. Alloys with 43 wt.% chromium or less tended to display discontinuous oxide formation and local spalling [2] when exposed to type I hot corrosion conditions (molten ash environment containing sodium sulfate and/or potassium sulfate at temperatures ranging from 850 to 950 °C). Alloys with higher chromium content tended to display thinner, more continuous surface oxides and less hot corrosion penetration into the alloy. On the other hand, nickel alloys containing more than 30% chromium are extremely difficult to fabricate by conventional hot working processes because of the development of a brittle alpha chromium phase. Once  $\alpha$ -Cr is present, the alloy is more difficult to work because  $\alpha$ -Cr is hard to deform and less ductile than  $\gamma$ -Ni. In addition, high-chromium nickel-based alloys are susceptible to a decrease in ductility after exposure to elevated service temperatures [2].

In recent years there has been a growing interest in the use of high velocity oxy-fuel (HVOF) thermal spraying for depositing protective coatings of various materials on a wide variety of substrates [3–5].

Coatings deposited by other thermal-spray processes had limited usefulness as corrosion protection coatings due to the presence of interconnected porosity in the structure. However, HVOF coatings can be produced with less porosity than other types of thermal-sprayed coatings and are now extensively studied for their corrosion-resistant properties [6].

Co-extruded INCOCLAD 671 / 800H tubing (a corrosion-resistant 50Ni–50Cr alloy clad on an alloy 800H core) has been used successfully in the heat-exchanger sections of coal-fired utility boilers since the early 1970's [7,8]. Furthermore, positive experience was reported on the use of 50Cr–50Ni as a metal dusting resistant coating [9]. An HVOF sprayed 50Ni–50Cr coating yielded good protection until 750 °C in ultra-supercritical (USC) boiler components [10].

The development of corrosion and erosion protective coatings using thermal-spray techniques requires in-depth knowledge of the principal characteristics of these products [11]. The heated and potentially molten, oxidized, or vaporized particles strike the substrate whereupon they deform (i.e., “splat”) and adhere through predominantly mechanical mechanisms [12]. Because the splat is rapidly quenched upon impact, the deposit may consist of an amorphous, microcrystalline, or fine-grained mixture of both thermodynamically meta-stable and stable phases [13].

The purpose of the present communication is to describe the complex microstructure of phases obtained by HVOF spraying of Ni–50Cr alloy, and to discuss the limitations of standard characterization techniques in analyzing such microstructures. To date, only a small number of studies have been reported in the open literature focused on

\* Corresponding author. Present address: 8th Floor, Bahen Building, 40 St. George Street, Toronto, Ontario, Canada M5S 3G8. Tel.: +1 416 635 5309; fax: +1 416 946 8252. E-mail address: [jahan.saaedi@utoronto.ca](mailto:jahan.saaedi@utoronto.ca) (J. Saaedi).

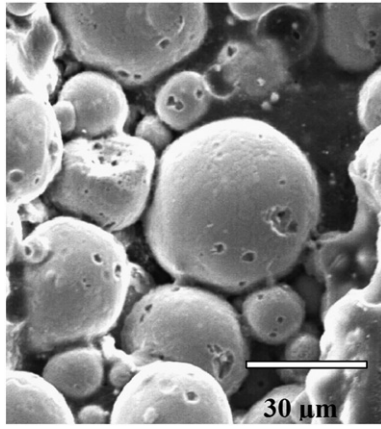


Fig. 1. SE image of AMDRY 350F powder.

the characterization of the microstructure and phase composition of HVOF sprayed coatings of Ni–50Cr and similar alloys. Most studies of coatings of this alloy have dealt with the evaluation of the performance of the coatings when exposed to environments typical of practical service conditions.

## 2. Experimental methods

The coatings were deposited by means of a Sulzer Metco DJ 2700 Diamond Jet Gun onto stainless steel plates to a thickness of approximately 200  $\mu\text{m}$ . Nitrogen was selected as the carrier gas and the fuel gas was propylene. Online diagnostic measurements were carried out using the Tecnar DPV-2000 diagnostic system to measure particle characteristics in-flight and better understand the deposit formation.

Powder particle size was determined using a Malvern Mastersizer particle size analyzer. Cross-sections of the powder particles were prepared by mounting the particles in resin and then grinding and polishing. Coated substrates were sectioned and polished for microstructural characterization using optical microscopy and scanning electron microscopy (SEM). Energy dispersive X-ray spectroscopy (EDS) analyses were performed during SEM examination. The scanning electron microscopes used in this work were a JEOL JSM-840 (SEM) complemented by a PGT/AAT EDS detector (thin window), and a Hitachi S-4500 field emission (FE-SEM) instrument.

The phase compositions of the powder and coatings were characterized by X-ray diffraction (XRD) using a Philips PW 2273/20 diffractometer with  $\text{Cu } K_{\alpha}$  radiation and a scanning rate of  $1.45^{\circ} 2\theta/\text{min}$ . The diffractometer was operated at 40 kV and 40 mA. The XRD analyses were conducted on a lightly compacted powder sample and the top as-deposited surface of the coatings. The lattice parameters of the powder and coatings were determined by calculating the lattice parameter from the three most intense fcc peaks in the XRD patterns, plotting these against  $\cos^2\theta/\sin\theta$ , and extrapolating the line of best fit to  $\theta=0$  to eliminate the effect of displacement error [14].

Line scans and semi-bulk elemental analyses on cross-sections of coatings were carried out by electron probe microanalysis (EPMA, Cameca SX50) using a Ni alloy (NIST certificate, SRM 1244–NiCr, 73Ni16Cr10Fe),  $\text{Cr}_2\text{O}_3$ , and NiO as standards. Spectra were recorded at 1  $\mu\text{m}$  intervals during the line scans. The semi-bulk analyses were carried out by collecting spectra from 10 to 12 non-overlapping  $40 \mu\text{m} \times 60 \mu\text{m}$  square areas on the coating cross section of each sample.

Clemex image analysis software was utilized in order to quantify the porosity level and oxide content in the coatings. Images for image analysis were obtained from as-polished surfaces using light microscopy, or secondary electron (SE) or backscattered electron (BSE) signals in the SEM. Heat treatments were carried out on coated samples at 650  $^{\circ}\text{C}$  for 1 and 4 h under vacuum ( $10^{-5}$  mb) in a Red Devil high temperature vacuum furnace.

## 3. Results and discussion

### 3.1. Ni–50Cr powder

Commercial Ni–50Cr powder from the Sulzer Metco Company (AMDRY 350F) was used for the study. The nominal composition of the alloy was Cr-49.6% C-0.03% Fe-0.1% Mn-0.1% Si-0.3% Ni-balance (in wt.%). A secondary electron image of the powder particles is shown in Fig. 1. The majority of the particles have a near-spherical morphology, typical of powder produced by inert gas atomization. The particle size distribution is shown in Fig. 2. The median particle size was 35  $\mu\text{m}$ ; 25 vol.% was smaller than 20  $\mu\text{m}$ .

### 3.2. HVOF spraying

A set of eight experiments with five variable factors was designed for the initial stage of process optimization. Oxygen flow, fuel flow, air flow, standoff distance, and feed rate were considered as the main controllable factors of the spray process. Particle velocity and particle temperature at the substrate position were selected as measurable outcomes. Table 1 summarizes the two most promising combinations of processing parameters, which were used to deposit the coatings characterized in this study. Among the eight experiments, the conditions used for Coating 2 produced the highest particle velocity along with a relatively low particle temperature. The fuel/oxygen ratio for Coating 2 was 0.28, which is fuel-rich and about 1.3 times the stoichiometric ratio of 0.22. The fuel/oxygen ratio was 0.17 (fuel-lean condition) for Coating 1, for which the particles had a lower velocity and lower temperature in-flight. However the difference in particle temperatures may be placed on the range of DPV standard error.

### 3.3. Optical microscopy

Optical micrographs of as-polished cross-sections of coatings are shown in Figs. 3 and 4. The coatings were extremely dense and the splats were wide and flat. The porosity levels of Coatings 1 and 2 were less than 1%, as measured by image analysis. In addition to the light contrast matrix of coating alloy, there were darker areas which occupied an extensive part of the microstructures. Some of these areas were very dark with a contrast close to that of the pores. More unmelted particles can be seen in Coating 1, suggesting lower particle temperatures during the spraying process.

### 3.4. X-ray diffraction

The diffraction pattern of the powder exhibited three peaks which could be assigned to the (111), (200) and (220) planes of  $\gamma$ -Ni. This

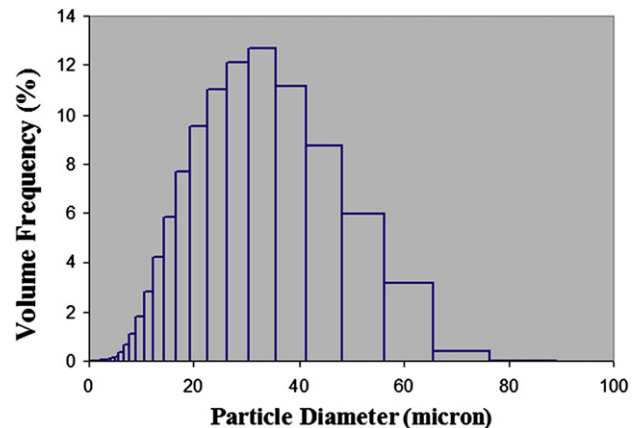


Fig. 2. Particle size distribution of used commercial powder particles.

Download English Version:

<https://daneshyari.com/en/article/1661281>

Download Persian Version:

<https://daneshyari.com/article/1661281>

[Daneshyari.com](https://daneshyari.com)